Supporting Online Material for

A Stochastic Single-Molecule Event Triggers Phenotype Switching of a Bacterial Cell

Paul J. Choi, Long Cai, Kirsten Frieda, X. Sunney Xie*

*To whom correspondence should be addressed. E-mail: xie@chemistry.harvard.edu

This PDF file includes:

Materials and Methods
SOM Text
Figs. S1 to S8
References

Other Supporting Online Material for this manuscript includes the following: (available at www.sciencemag.org/cgi/content/full/322/5900/442/DC1)

Movie S1

Supporting Online Material

MATERIAL AND METHODS

Strains and media

Strains were constructed using standard molecular biology techniques. PCR amplification was performed using on a YFP-kanamycin resistance cassette identical to the one in SX4 (*S1*) as a template. PCR was performed with primers containing overhangs targeting the desired homologous recombination by the lambda-Red system (*S2*), so subsequent electroporation into BW25993/pKD20 generated strain SX700. Similar PCR amplification of the Tsr-YFP-kanamycin cassette using strain SX4 as a template generated strain SX701. N. Friedman and J. Hearn provided plasmid pSX704, consisting of a *lac* operon region with O2 and O3 mutated to non-operator sites inserted into the pKO3 vector (*S3*). In removing the O3 operator, the CAP binding site was unperturbed in order to maintain the same effect of CAP on the promoter of all the strains. A two-step homologous recombination of pSX704 with SX700 followed by screening of the crossover site generated strain SX702. Strain and primer sequences are available on request.

Liquid cultures where shaken at 37 °C in M9 minimal media supplemented with 0.4% glycerol, amino acids, and the specified amounts of methyl- b-D-thiogalactoside (TMG).

Microscopy

Overnight liquid cultures were rediluted 100-fold in new media and grown to OD600 = ~0.1. For single-timepoint analysis, ~1 mL of the culture was pelleted by centrifugation, resuspended in ~10 uL of new media, and ~1 uL placed between two cleaned glass coverslips for imaging. For time-lapse movies, cells were pelleted and resuspended in ~50 uL of new media. Then, ~0.5 uL was placed between a 3 % agarose gel (Seaplaque) pad made with media and a glass coverslip, before assembling a imaging chamber (Bioptechs, FCS2) heated at 37 C. TMG was included in the gel pad, and a flow of fresh, prewaremd media containing TMG was also provided with a peristaltic pump at 1 mL/min. We found that continuous flow of fresh media containing inducer was necessary to provide consistent results. Images were recorded on an inverted microscope (Olympus, IX-71) with a 100x oil immersion phase contrast objective (Olympus, NA=1.35) and CCD camera (Andor, Ixon). The microscope provided an additional 1.6x internal magnification.

For single-molecule movies, a 50 ms exposure was followed immediately by 3 additional images provided photobleaching of existing fluorophores. Examination of these photobleaching images showed that the majority of fluorophores were photobleached. Excitation was provided by an Ar-Kr laser (Coherent, Innova Sabre) at 514 nm with an intensity of ~1 kW/cm^2. For induction time-lapse movies and high expression analysis,

excitation was provided by a mercury lamp (Olympus) with 300 ms exposures. Image acquisition was controlled with Metamorph software (Universal Imaging).

Data analysis

Data analysis was done though a combination of manual and automated analysis using Metamorph and custom software for Matlab (The Mathworks, Inc.). Phase contrast images were used to identify cell boundaries and the corresponding pixels from the fluorescence image used to calculate integrated cell fluorescence intensities, normalized by cell size, to construct histograms for single time-point analysis. For single molecule analysis, the number of spots provided the total number of molecules. In the case of overlapping molecules (as in the case of Tsr which oligomerizes), intensities of a 3x3 pixel square centered on the maximal peak of fluorescence intensity was used to determine the total number of molecules. The integrated fluorescence intensity for cells with 0 to 4 molecules, averaged over many cells, was plotted to obtain a calibration for the absolute number of YFP molecules at high levels of expression based on integration alone, as further described in the Supplemental Data. This allowed an estimate of absolute molecule numbers at high expression. For analysis of time courses for inducing cells, automatic cell segmentation was not sufficient to identify individual cells in microcolonies. Average fluorescence intensities were determined by manually highlighting cells and subtracting the background from a nearby region of pixels. For *a-b* analysis of distributions from the integrated intensity, such as in Figure 3D, a strain lacking YFP was used to subtract the mean and standard deviation due to autofluorescence. The distributions plotted in Figure 3D were obtained by deconvolution of the autofluorescence histogram with the observed fluorescence histogram using Matlab and a FFT method.

LacZ assays

β-galactosidase activity of the LacY-YFP fusion strain as compared with the parent strain in Figure S1 was analyzed using a fluorometer (Fluorolog, Jobin Yvon Spex). Cells were grown to log phase under varying concentrations of TMG. Addition of 10% chloroform by volume and vortexing for 5 seconds served to permealize them. The fluorogenic substrate, fluorescein di-β-D-galactopyranoside (FDG), was then added to a final concentration of 150 μM. β-galactosidase catalyzed hydrolysis rates were calculated from the slope of fluorescence increase.

Measurements of LacZ activity for Figure S6 were carried out using a spectrophotometer (Beckman Coulter, DU800) and a modified Miller assay with reagents and protocol from Pierce Biochemical.

Estimation of absolute permease numbers at high concentrations

The number of LacY-YFP determined by manual counting of single-molecules was

compared with the integrated fluorescence intensities for the same cells to provide a calibration of total cell fluorescence and absolute molecule numbers when using high-power, laser excitation, as shown in Figure S5, which was then extrapolated to high copy numbers. A fully induced sample was used as a control to calibrate the relative fluorescence intensities of laser and lamp excitation, allowing estimation of absolute numbers at high copies using lamp excitation.

To check the accuracy of the estimation, we note that single-molecule counting under laser excitation gives an average of one molecule in the uninduced state, and our calibration for the lamp measurement gives an average of about one thousand molecules after full induction. This thousand-fold induction agrees with our independent measurement by a Miller assay of a thousand-fold induction (*S4*). Even with an error in the estimate of absolute numbers, it is clear that the number of permease molecules necessary to force a change in phenotype is about two orders of magnitude greater than the mean number of permease molecules for uninduced cells.

SUPPLEMENTAL TEXT

Properties of LacY as a reporter and comparison with Tsr

The single-molecule measurements in strain SX700 and SX701 in media lacking inducer yielded similar values for both the mean and variance of protein expression. SX700 has an average of 0.9 molecules/cell and a standard deviation of 1.4 molecules/cell. In comparison, SX701 has an average of 1.0 molecules/cell and a standard deviation of 1.5 molecules/cell. This suggests that Tsr and LacY have similar efficiencies for translation, folding, and membrane insertion, as well as similar stability towards proteolysis. Thus, the use of Tsr as a reporter of promoter activity in the presence of inducer is justified. The similarity of Tsr and LacY results also showed that LacY dimerization was insignificant for the low copy numbers probed and did not affect the counting.

Cell membrane permeability of TMG

Our conclusions rely on the fact that TMG can diffuse into the cell even in the absence of permease molecules. Such diffusion of TMG provides a low concentration that is sufficient to sequester LacI that is dissociated from its operators (*S7, S8*). Previous measurements of TMG permeability support our conclusions. After 30 minutes of incubating permease-deficient cells with 25 μM TMG, measurement of TMG accumulation showed that the intracellular TMG concentration matched the extracellular TMG concentration (*S5*). Another measurement of TMG transport in permease-deficient cells found that the intracellular TMG reached an equilibrium level within several minutes (*S6*). From these two reports, we can conclude that the intracellular and extracellular TMG are similar and equilibrate within several minutes. Thus, in the presence of extracellular TMG in the range of 20-50 μM, we can expect a similar intracellular TMG concentration that can sequester cytoplasmic LacI and assist in

generating large bursts.

As a final note, Figure S6 clearly shows that TMG can penetrate the cell membrane and induce expression from the *lac* promoter in the absence of permease transporters.

Why one permease molecule is not enough to induce

We claim that the small number of permease molecules observed in uninduced cells (Fig. 1D) indicate that the threshold for induction must be much higher than ten molecules and argue that if one permease were enough, uninduced cells would contain zero permease molecules. The possibility that these cells are in a slow intermediate deterministically leading to induction is ruled out for two reasons. First, Figure 1C indicates that the timescale of induction is about one day. That is, a cell can spend one day in the uninduced state before transitioning into the uninduced state. The timescale of stochastic protein production and dilution from cell division in the uninduced state is about one hour. Thus, a cell will lose memory of how many molecules it has over the course of several hours because of the stochasticity of protein production. It would be impossible for a cell with one permease molecule to maintain a state of one permease molecule, or deterministically increase slowly over the course of one day, since the size of noise is larger and timescale of noise is faster.

Of course, the data in Figure 2 provides independent support of our claim regarding the threshold.

The change in repression ratio from eliminating looping is insufficient to cross the threshold

Eliminating looping in strain SX702 causes a very large change in the switching rate. Eliminating looping also causes a decrease in repression. However, the increased permease expression from the change in the repression is insufficient to cross the threshold. In the absence of permease feedback, the distribution in Figure 3D shows that the change in repression, even in the presence of 50 uM TMG, is too small for cells to cross the threshold of 375 molecules. However, Figure 2D shows that even at as low as 20 uM TMG, all cells show rapid, uniform induction.

Figure 2A further shows that even if a cell contains one or two hundred permease molecules, in the presence of looping, induction is unlikely. Such cells have even more permease molecules than would be caused by the change in repression. However, looping still prevents these cells from inducing.

Thus, a direct comparison of cells with identical numbers of permease molecules but different looping states shows that looping does indeed cause change the rate of switching by orders of magnitude, and the resulting increased permease levels caused by the absence of looping is insufficient to activate positive feedback.

Bursting properties of the *lac* promoter

The burst-like nature of gene expression in *E. coli* has been reported in three different scenarios: the fully repressed *lac* operon (*S1, S9*), the fully induced *lac* promoter (*S10*), and during the induction of the *lac* operon (this report). These three bursting processes result from distinct, but related, mechanisms as we describe below.

The burst-like production of proteins observed from the repressed *lac* operon in previous reports resulted from the translation of multiple proteins from a single transcript (*S1, S9*). These experiments were carried out for uninduced cells in the absence of inducer. Previously, the result was interpreted as the dissociation and rapid rebinding of the lactose repressor from its operators, allowing enough time for a single transcription event. We extend the previous interpretation by arguing that each dissociation event leading to the observed transcription is in fact only a partial dissociation event, and not a complete dissociation event.

We expect that a complete dissociation event would lead to multiple rounds of transcription, generating a different kind of large bursting. Why were large bursts resulting from complete dissociations not observed in the previous reports? Complete dissociation events occur with a frequency that is orders of magnitude smaller than partial dissociation events. The frequency of partial dissociation events leading to transcription was about once per cell cycle. The probability of observing a complete dissociation event would be too small to appear in the results. Furthermore, these experiments were carried out in the absence of inducer, which we argue is necessary for creating very large bursts through sequestration of the lactose repressor once it dissociates from its operators.

Another observation of bursting at the transcriptional level was reported for a fully induced *lac* promoter (*S10*). In the previous report, the function of the repressor is irrelevant, because the system is saturated with a high concentration of inducer. The mechanism behind the transcription bursting in the absence of repressor function is unknown. In the present report, though, we discuss a different kind of large bursting behavior that is repressor-dependent. Large bursts of multiple transcripts occur because of the rare, complete dissociation of the lactose repressor and slow rebinding time in the presence of moderate amounts of inducer.

Application of *a-b* bursting model to low and high protein expression

The interpretation of $a = \mu^2/\sigma^2$ and $b = \sigma^2/\mu$ as the number of transcripts per cell cycle and proteins per mRNA, respectively, was presented and validated for protein distributions from the repressed *lac* promoter (*S9*). Under repressed conditions, the partial dissociation of the tetrameric repressor leads to single transcripts, as proved in Reference S1, validating the interpretation of *a* and *b* as translational bursts for single mRNA.

However, as noted in Reference S11 and also discussed in Reference S12, the interpretation of a and b can be generalized to the case of multiple transcripts per bursting event. This interpretation is valid if the period of transcriptional activity results in a total number of proteins that are exponentially distributed per burst, even if the proteins result from multiple transcripts. Then, a corresponds to the frequency of these multi-transcript events, and b to the aggregate number of proteins per event. This scenario could likely exist, for example, for a repressor that dissociates and remains dissociated for an exponentially-disributed amount of time, during which a proportional number of mRNA are generated.

In this example, a corresponds to the frequency of repressor dissociation, while b corresponds to the total number of proteins per "large burst". Because the gamma distribution behaves as the convolution of a exponential distributions with average size b, the application of the model, whether a and b correspond to single transcripts or large, effective bursts, remains valid, if the bursting behavior can be approximated as the sum of events with exponentially-distributed sizes.

The interpretation of a and b as burst frequency and size parameters can be difficult at high expression levels, when extrinsic noise or other factors can dominate the protein noise, rather than the bursting process. However, we have observed that strong promoters including the fully induced *lac* operon have similar values of $a = \mu^2/\sigma^2 \approx 10$, and rarely above that. Thus, $a \approx 10$ may be a limit on protein noise imposed by extrinsic noise. However, below this, the interpretation of a is likely to be valid. Because we measure $a \approx$ 3-4 for the large bursts in Figure 3D, the interpretation of a as the burst frequency is better supported.

Direct burst size distribution in the presence of DNA looping and inducer

Figure 3B shows the burst size distribution determined for the data collected for the real-time traces in Figure 3A for over 200 bursts. The vast majority of the bursts (93%) have a size smaller than 10 molecules, which are well fit by an exponential distribution as predicted and observed previously (*S1, S9*). However, looking at the complete distribution shows a number of very large bursts that are not well-fit by the previous exponential distribution. The Z-score of the largest bursts range from 10 to over 200, using the mean and standard deviation of the exponential fit. The extremely large Z-scores support our interpretation of the large bursts arising from a separate physical mechanism, complete dissociations, from the small bursts, which are well-fit by an exponential distribution. Although obtaining a burst size distribution for these infrequent events is difficult, we do observe that the largest burst size observed is 250 molecules, which is a similar order of magnitude to the permease threshold measured in Figure 2. Such extremely large bursts are not observed in the absence of inducer (for example, in Reference S1).

Role of inducer in LacI dissociations and large bursts

Our model describes a single event – the complete repressor dissociation – as the event trigger a change in phenotype. The rate of phenotype switching has a dependence on inducer concentration, as evident from Figure 1C, so the complete dissociation events must be influenced by inducer. We consider here the possible role of inducer on complete dissociation events.

A key fact is that LacI repressors bound to their operator sites have lower binding constants for inducers like TMG than free LacI (*S7, 8*). The lower binding constant results from a combination of slower association rate and faster dissociation rate of TMG with LacI. At sufficiently high inducer concentrations of about 1mM, TMG can associate to LacI still bound to its operators and force a complete dissociation event. This situation occurs once a cell is fully induced with many permease molecules actively transporting TMG. The cells shown in Figure 2 initially have LacI bound to their operators at the initial time. Figure 2B shows that ~375 permease molecules concentrates TMG high enough to force a complete dissociation of LacI still bound to DNA.

Our conclusion, though, is that such forced dissociation events do not trigger phenotype switching, but only occur once the decision to change has already been made. We note that the binding constant of free LacI for TMG is in the range of 10-100 μM, which is precisely the range of bistability. Thus, in this range, once LacI spontaneously dissociates from all of its operators, it can be sequestered by 10-100 μM to generate a large burst of permease expression. It is still possible that a partially-dissociated repressor may interact with inducer, but it is unlikely for inducer to interact with a repressor head already bound to its operator.

While the inducer is unlikely interacting with fully-bound tetrameric repressor, once a dimer head dissociates, it could conceivably bind to inducer. Thus, inducer could increase the length of time of this partially-dissociated state, which would increase the probability of one RNA polymerase binding, such as demonstrated by the slight increase in burst frequency in Figure 3C. However, because the duration of each partial dissociation event is still much shorter than transcription initiation rates, only one RNA polymerase can bind and transcribe.

Since a partial dissociation is an obligatory intermediate step for a complete dissociation, stabilization of the partially-dissociated state would increase the rate of complete dissociation, but by no more than a similar factor of two. This is still not "pulling off" the bound repressor, but waiting for at least one dimer head to spontaneously dissociate.

We also point out that although the frequency may increase by only a factor of two, the induction rate increases a dramatic amount across the same TMG concentration range, as shown by the concentration dependence of the bimodal distributions in Figure 1C. The inducer may increase both the burst size (by sequestration) and burst frequency (by interacting with partial dissociations). However, since the small burst frequency only

increases by a factor of two, we argue that the dominant factor behind the concentration dependent transition rate is likely the burst size and sequestration.
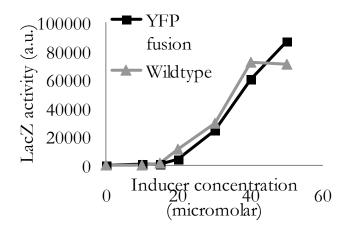
Does every complete dissociation event lead to a phenotype transition? What does this mean for our model?

Following a complete dissociation, if enough permease molecules are generated, the resulting influx of inducer will be high enough to sequester the repressor permanently, and "pull off" the repressor if it does rebind (as in Figure 4A).

If, however, not enough permease molecules are made, the repressor will rebind to its operators, and the inducer concentration will be too low to "pull off" the repressor from its operators (otherwise there would be permanent induction). Then, the frequency of complete dissociations should not be changed by more than the factor of two previously discussed. The next large burst will occur randomly and be uncorrelated with the fact that a complete dissociation has recently occurred.
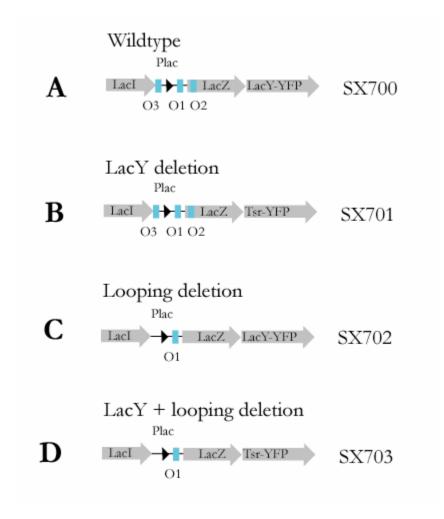
Thus, multiple complete dissociations may occur before a phenotype transition. However, each complete dissociation event will be a random, uncorrelated event, and the frequency of complete dissociations is very low (much less than the cell cycle). The effects of individual bursts will not be cumulative, as in the traditional model of protein noise crossing the threshold for positive feedback. The traditional model of protein noise invovles a many-step random walk, where the effect of new protein expression builds on the past protein production. Rather, the transition across the threshold will still be one large expression event, uncorrelated with prior expression events. This is the key point of our model, which means that a single molecule event will still control the phenotype transition, rather than protein noise resulting from the combined effect of many repressor dissociation events.

SUPPLEMENTAL FIGURES

Figure S1. Permease activity of fusion protein
Induction of strain SX700 carrying a LacY-YFP fusion and the parent strain containing wildtype LacY are identical, indicating that the permease function is not perturbed by the YFP tag. Induction was measured with a fluorogenic hydrolysis assay using the substrate fluorescein-di-β-D-galactopyranoside.

Figure S2. Srains used in this study.
(A) Strain SX700 encodes a LacY-YFP fusion with intact wildtype regulatory elements. (B) Strain SX701 replaces the lactose permease gene with the membrane protein fusion, Tsr-YFP, eliminating positive feedback from permease transport. (C) Strain SX702 lacks the auxiliary operators O2 and O3. Every dissociation of the tetrameric repressor from its single operator will result in a complete dissociation. (D) Strain SX703 contains eliminates both looping and permease function.
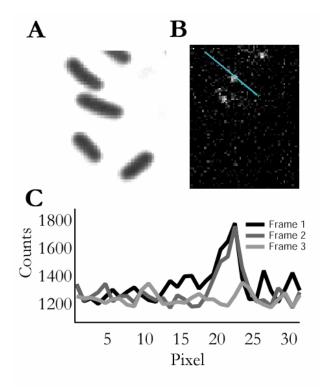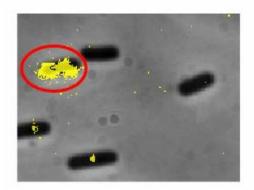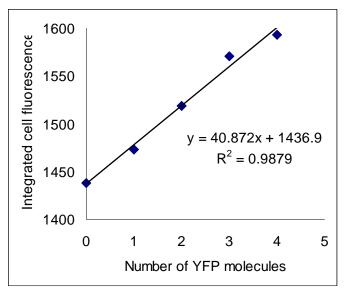
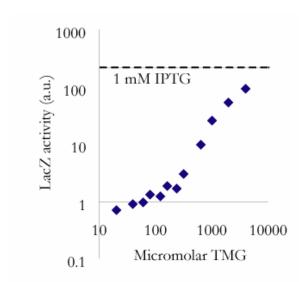**Figure S3**. **Single cell detection of LacY-YFP**
A) Phase contrast image of *E. coli* cells. (B) Corresponding fluorescence image of single LacY-YFP molecules in uninduced cells. (C) Linescan of cell fluorescence for blue line in (B). Subsequent image acquisitions demonstrate single step photobleaching of the LacY-YFP molecules.

Figure S4. Strain SX701 replaces the lactose permease gene with the membrane protein fusion, Tsr-YFP, eliminating positive feedback from permease transport. After incubation in moderate amounts of TMG (50 μM TMG shown here), the majority of cells contain several YFP molecules, but cells containing much more YFP molecules are occasionally observed, as circled in red.
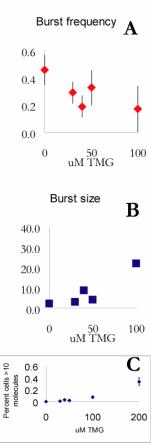
Figure S5. Absolute calibration of integrated fluorescence intensities
A linear fit of integrated fluorescence intensities (normalized by size) for cells containing 0 to 4 molecules provided a calibration for estimating YFP numbers at higher expression levels.
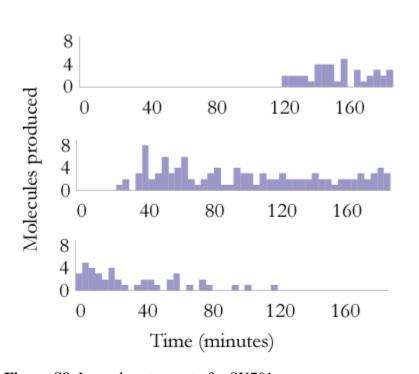

Figure S6. Induction of permease-deficient strain SX701 using ONPG assay for LacZ activity. Cells were incubated with TMG for a minimum of 12 hours before measurements. Even in the absence of specific permease transport, cells show an induction response to TMG. The average expression does not increase significantly below 500 μM TMG. In contrast, the induction rate for SX700 increases dramatically between 0 to 50 μM TMG. This suggests that the binding constant for TMG is too low to affect operator-bound repressors within the bistable concentration range, but that the TMG can interact with free repressors to assist with induction. The dual binding

constants of inducers for operator-bound and free repressor were measured in References S7 and S8.

Figure S7. Burst properties of SX701.
The burst properties of permease-deficient SX701 were determined from the complete steady-state distribution (including cell with greater than ten molecules). (A) The burst frequency, calculated as the inverse of the coefficient of variation. (B) The burst size, calculated as the Fano factor. The interpretation of burst size and frequency is complicated by the presence of both small and large bursts. However, the increase in Fano factor is consistent with a greater contribution from the large bursts. (C) The percentage of cells with more than 10 molecules increases as TMG concentration increases. The rare occurrence of these high expression cells makes their quantitative characterization difficult.

Figure S8. Large bursts events for SX701.

Three additional examples of large burst events for SX701 in the presence of 200 μM TMG are shown, similar to Figure 3A.

SUPPLEMENTAL MOVIE

Movie S1. Fluorescence overlay on phase contrast time-lapse. One daughter cell of a dividing cell switches its phenotype and expresses many LacY-YFP molecules, while the other daughter does remains in a phenotype with low expression. Cells were immobilized with polylysine in a flow cell with a continual flow of fresh M9 minimal media supplemented with amino acids and 50 μM TMG. Each frame of the movie corresponds to a 2 minute time-lapse.

SUPPLEMENTAL REFERENCES

S1. J. Yu, J. Xiao, X. Ren, K. Lao, X. S. Xie, *Science* **311**, 1600-1603 (2006).

S2. K. A. Datsenko, B. L. Wanner, *Proc. Natl. Acad. Sci. U.S.A.* **97**, 6640-6645 (2000).

S3. A. J. Link, D. Phillips, G. M. Church, *J. Bacter.* **179**, 6228-6237 (1997).

S4. S. Oehler, E. R. Eismann, H. Krämer, B. Müller-Hill, *EMBO J.* **9**, 973-979 (1990).

S5. J. L. Flagg, T. H. Wilson. *J. Bacter.* **128**, 701-707 (1976).

S6. E. A. Matzke, L. J. Stephenson, R. J. Brooker, *J. Biol. Chem.* **267**, 19095-19100 (1992).

S7. M. Dunaway, J. S. Olson, J. M. Rosenberg, O. B. Kallai, R. E. Dickerson, K. S. Matthews, *J. Biol. Chem.* **255**, 10115-10119 (1980).

S8. M. D. Barkley, A. D. Riggs, A. Jobe, S. Bourgeois, *Biochem.* **14**, 1700-1712 (1975).

S9. L. Cai, N. Friedman, X. S. Xie, *Nature* **440**, 358-362 (2006).

S10. I. Golding, J. Paulsson, S. M. Zawilski, E. C. Cox, *Cell* **123**, 1025-1036 (2005).

S11. N. Friedman, L. Cai, X. S. Xie, *Phys. Rev. Lett*. **97**, 168302 (2006).

S12. L. Cai. Thesis. Harvard University.